ANNUAL REVIEWS

Annual Review of Analytical Chemistry

Mass Spectrometry Measurements of Neuropeptides: From Identification to Quantitation

Eduardo A. De La Toba,[1,2,*] Sara E. Bell,[1,2,*] Elena V. Romanova,[1,2] and Jonathan V. Sweedler[1,2]

[1]Department of Chemistry, University of Illinois Urbana-Champaign, Urbana, Illinois, USA; email: jsweedle@illinois.edu

[2]Beckman Institute for Advanced Science and Technology, University of Illinois Urbana-Champaign, Urbana, Illinois, USA

Annu. Rev. Anal. Chem. 2022. 15:83–106

First published as a Review in Advance on March 24, 2022

The *Annual Review of Analytical Chemistry* is online at anchem.annualreviews.org

https://doi.org/10.1146/annurev-anchem-061020-022048

*These authors contributed equally to this article.

Keywords

neuropeptide, quantitation, mass spectrometry, ion mobility spectrometry, imaging, single cell

Abstract

Neuropeptides (NPs), a unique class of neuronal signaling molecules, participate in a variety of physiological processes and diseases. Quantitative measurements of NPs provide valuable information regarding how these molecules are differentially regulated in a multitude of neurological, metabolic, and mental disorders. Mass spectrometry (MS) has evolved to become a powerful technique for measuring trace levels of NPs in complex biological tissues and individual cells using both targeted and exploratory approaches. There are inherent challenges to measuring NPs, including their wide endogenous concentration range, transport and postmortem degradation, complex sample matrices, and statistical processing of MS data required for accurate NP quantitation. This review highlights techniques developed to address these challenges and presents an overview of quantitative MS-based measurement approaches for NPs, including the incorporation of separation methods for high-throughput analysis, MS imaging for spatial measurements, and methods for NP quantitation in single neurons.

INTRODUCTION

The discovery of neuropeptides (NPs) is rooted in the extensive and groundbreaking research performed by scientists in the fields of pharmacology, physiology, and endocrinology during the late nineteenth and early twentieth centuries. However, it was not until 1971 that the term neuropeptide was formally introduced to describe short peptides capable of inducing physiological responses. This novel class of endogenous signaling molecules shares certain unique characteristics, including their biosynthesis from larger precursor polypeptides, and their storage in large dense-core secretory vesicles as opposed to small secretory vesicles of classical neurotransmitters (1). In this review, we use the term neuropeptide when referring to peptides that act locally in the nervous system and also peptide hormones that act at distant targets; often, the same peptide may perform both roles, depending on the context, making their distinction difficult. Importantly, NPs are promiscuous ligands with high receptor-binding affinities, possessing K_D values in the nanomolar to micromolar range, enabling them to exert their biological functions at several orders of magnitude lower concentrations than classical neurotransmitters. Since the adoption of the term, hundreds of NPs, often conserved across the animal kingdom, have been discovered and shown to regulate a broad range of biological functions (2). Select examples of NPs and their endogenous roles include orexins, which are involved in wakefulness and food intake, substance P and its role in nociception, and vasopressin, which regulates osmolality and vasoconstriction (3–5).

Given the functional diversity of NPs, they are often prime candidates for studying various neurological, psychological, and metabolic disorders (6, 7). Currently, there are over 70 US Food and Drug Administration (FDA)-approved drugs that target specific NP receptors or pathways, with insulin being perhaps the most well known (8). NPs are broadly localized throughout the central and peripheral nervous and neuroendocrine systems (2). Quantitative analyses of NPs in these tissues and cellular releasates help us understand NP differential regulation in response to environmental or pharmacological stimuli and diseases. Additionally, with the emergence of single neuron–based NP measurements and improvements in single-cell sampling techniques, quantitative analyses may provide valuable information regarding cellular heterogeneity and NP dynamics in a neuron-specific manner (9). Here, we present an overview of modern approaches for NP characterization and quantitation powered by cutting edge mass spectrometry (MS) technology.

STRATEGIC MEASUREMENT AND QUANTITATION APPROACHES

A unique aspect of NP detection is that multiple NPs may be produced from one gene via posttranslational enzymatic processing of the encoded precursor protein, typically referred to as a prohormone (10). Therefore, probing DNA and messenger RNA (mRNA) transcripts does not provide information regarding the complexity of peptide products, especially as it does not capture the variety of posttranslational modifications (PTMs) often present on mature NPs. Because these modifications can change the function and lifetime of peptides, having knowledge of them is often important. Well suited for the discovery of potentially novel NPs, MS measures NPs in a nontargeted manner without the use of molecular probes and does not require prior information on analyte structure. These measurements provide unambiguous identification of NPs based on the mass-to-charge (m/z) ratios of their ions in the gas phase, as well as their unique molecular fragmentation patterns, thereby allowing elucidation of NP structural details. With the development of MS instruments capable of high-resolution m/z measurements, mass accuracy measurements in the parts-per-billion (ppb) range become feasible, enabling the discernment of isobaric ions for reliable assignment of known peptides by mass and isotopic patterns (11). Additionally, when coupled to analytical separations, such as liquid chromatography (LC), capillary electrophoresis (CE), and ion mobility spectrometry (IMS), MS offers significant improvements in detection capacity

by reducing sample complexity prior to measurement (12). Furthermore, the development of MS imaging (MSI) techniques has enabled the visualization of NP distribution within tissues through direct tissue measurements, both qualitative and quantitative, without the need for NP-specific antibodies (13).

Given the rapid development of MS platforms with limits of detection approaching 10 amol and fast scan speeds of up to 100 spectra per second, MS has emerged as a powerful analytical technique for neuropeptidomics, the global characterization of NPs in a biological sample (14, 15). MS-based analyses can be broadly classified into targeted and global approaches, and quantitation is performed with or without chemical labeling. NP quantitation by MS is often aided by the front-end analyte separation platforms noted above, usually LC and CE, with IMS becoming more commonly incorporated into MS workflows. In what follows, the issues with more standard MS quantitation approaches are outlined, followed by the various LC-MS-based strategies that are effective for NP quantitation.

CHALLENGES FOR MASS SPECTROMETRY–BASED QUANTITATION

Quantitative NP analysis in neuronal tissue often yields valuable information regarding the diverse roles of NPs in various physiological processes and disorders. However, quantifying NPs by MS does present challenges; some are inherent to MS and several others are unique to NP biology and the sampling methods used.

Biological Factors Influencing Quantitation

Tissue collected for NP analysis may not reflect NP in vivo localization and concentration. Several factors contribute to these discrepancies, including regulated transport of NPs to peripheral release sites far from the origin of synthesis and postmortem protein degradation. Brain and other tissues have the ability to rapidly degrade NPs for termination of their signals after release (16). Postmortem protein degradation, in particular, must be controlled during tissue sampling because massive proteolysis of ubiquitous and structural proteins increases the dynamic range of biochemical concentrations and often obscures NPs, thereby limiting their detection and quantitation (17). Because postmortem proteolysis begins seconds after animal sacrifice, fast and effective tissue stabilization is crucial for preservation of the in vivo, neurochemical state. Various techniques have been developed for tissue stabilization, including, but not limited to, focused microwave irradiation, tissue boiling, adding protease inhibitors, and convective heating (18, 19). Comparative studies show that rapid heating is currently one of the more efficient tools for halting postmortem proteolysis and preserving intact NPs (20).

Localization of NPs to a subpopulation of peptidergic neurons within neural tissues poses challenges for sampling (21). While the concentration of an NP within an attoliter-containing dense-core secretory vesicle may be in the millimolar range, the effective local concentrations in many tissues are in the nanomolar to femtomolar range. Their sparse cellular localization dilutes peptide amounts in collected tissue extracts even further (22). As a result, tissue samples may contain NP concentrations spanning 6 to 10 orders of magnitude (23). This makes quantitative studies challenging because endogenous NP levels, typically between 3 to 5 orders of magnitude, may fall outside of the linear dynamic range of the mass spectrometer (24). Wide NP concentrations within a sample are problematic for MS quantitation, as these could lead to space-charge effects, which reduce the linear intra-scan dynamic range of the instrument, effectively masking the signal from trace NPs. Space-charge effects arise mainly from coulombic interactions between ions, and are especially pronounced in trap-based mass analyzers used in ion trap, Orbitrap, and ion cyclotron resonance mass spectrometers. These effects may reduce ion trapping

capacities, distort peak shapes from ions with similar *m/z* values, and reduce mass accuracy and sensitivity, making quantitation of lower level peptides in complex samples difficult (25). Thus, depending upon sample complexity and peptide concentrations, alternative mass analyzers, such as quadrupole time-of-flight, may be advantageous (26). Additionally, due to low endogenous amounts of certain NPs, a larger amount of tissue is often required to achieve adequate sensitivity for quantitation, which may prove impractical when analyzing tissue-limited samples. Larger samples are typically chemically complex, with salts, lipids, and metabolites present at higher levels than many NPs, further contributing to ion suppression (27). Off-line sample cleanup and purification steps are often incorporated to improve sensitivity and precision for quantitation.

Standard quantitation methods also prove challenging. For most bottom-up proteomic approaches, proteins are digested by trypsin, and individual peptides from the proteins are measured. Most software packages designed for proteomic quantitation rely on multiple tryptic peptides to infer protein abundance in a sample, e.g., by summing the top three largest peptide areas or taking the median of peptide ratios for a given protein (28, 29). For NPs, the levels of each peptide may be distinct and do not necessarily track each other. Tissue-specific processing of prohormones often arises from differences in the distributions of prohormone processing enzymes, leading to differences in the localization of NPs derived from the same precursor. For example, proopiomelanocortin produces over 10 unique NPs with various anatomical distributions (30). In addition, because distinct peptides from a prohormone may have different biological roles, quantifying the levels of the prohormone protein is rarely the goal. Thus, software that quantifies proteins based on combining the measurements of multiple peptides may not be useful for NP studies.

This is also why prohormone transcript quantitation may not be ideal for probing in vivo NP concentrations. Transcript levels do not necessarily correlate with prohormone levels due to multiple factors, such as translational regulation of mRNA, half-life differences between transcripts and the encoded prohormones, and neuronal polarity, which may cause spatially distinct (typically millimeters to centimeters) localization between transcripts and prohormones after transport of the prohormone away from the neuron soma to remote release sites (31). Accordingly, NP quantitation must be performed at the individual peptide level with direct measurement of mature NPs and their PTMs after prohormone processing.

Challenges with Statistical Processing of Mass Spectrometry Data

An important step in global, quantitative NP studies is post-MS statistical processing of raw data, including missing value imputation, peak intensity/area normalization, and multiple hypothesis-testing corrections. Because NP quantitation is often performed at the single-peptide level, missing peptide measurement values, e.g., ~20–50% of the peptide features in a typical LC-MS data set, are problematic for global NP quantitation (32). This presents unique challenges for quantitation, including reduced statistical power or preventing certain downstream statistical analyses. Missing peptide features often arise from biological factors; either the peptide is truly absent or below the detection limit of the instrument (not missing at random). Technical factors can also play a role, such as poor ionization and fragmentation, resulting in low-quality MS2 spectra (33). Several approaches developed for missing peptide imputation have been reviewed (34, 35).

Differential analysis of NPs often involves determining which peptides are significantly elevated or decreased in a particular condition relative to a control. When performing significance tests for hundreds or thousands of peptides in an MS experiment, multiple hypothesis-testing corrections are crucial. As the number of significance tests is increased, the number of peptides that pass the significance threshold will also increase simply by chance, resulting in multiple false positives (36). Therefore, multiple testing corrections aim to control either the false discovery rate

(FDR) or the familywise error rate by limiting the number of false positives that pass the significance threshold. Compared to the FDR, familywise error rate approaches may be excessively stringent, resulting in too few peptides considered significantly different. FDR-based approaches are typically more suitable for the exploratory nature of peptidomic analyses, as a more optimal balance between false positives and false negatives can be achieved (37).

TARGETED MASS SPECTROMETRY QUANTITATION

Targeted quantitation is a hypothesis-driven measurement of previously selected peptides for the purpose of comparing their levels under experimental conditions. This experimental design requires substantial knowledge about the presence of NPs in the sample and details about NP structural characteristics. For targeted NP quantitation, multiple-reaction monitoring (MRM) is perhaps one of the most commonly employed techniques, offering high precision, high sensitivity, and high throughput (38, 39). It is also important to define two types of quantitative measurements in the field of MS: A quantitative measurement provides relative quantitation between samples, whereas absolute quantitation provides an absolute amount (or concentration) of peptide.

MRM-based quantitation is conducted by selecting multiple *m/z* ratios of a peptide and its corresponding product ions, referred to as *m/z* transitions, with usually the most intense ion transition serving as the quantifier ion, and several transitions serving as qualifier ions. Quantitation is performed by integrating the peak area of the quantifier transition, whereas the qualifier ions serve to verify the identity of the analyte. The ability to deal with complex samples using MRM arises from three requirements for analytes to reach the MS detector: Analytes must be detected at the specified retention time and have both the specified precursor and fragment *m/z* ratios (40). These requirements ensure specificity, as detection is dependent upon multiple user-specified transitions unique for each monitored peptide sequence. The sensitivity of MRM-based assays is from a lower background and greater MS instrument observation time dedicated to peptide-specific transitions observed within a narrow retention time window. Typically performed on a triple quadrupole mass analyzer, which offers relatively low resolution [<5,000 full width at half maximum (FWHM)] and mass accuracies compared to high-resolution mass analyzers (10,000–1,000,000 FWHM) (41), MRM is suitable for quantitation of known NPs. However, distinguishing isobaric or structurally similar compounds that coelute with the targeted peptide may be difficult. For example, the C-terminal amidation PTM produces a mass shift of only −0.98 Da from the carboxylated peptide. Unless a sufficiently narrow mass window is used for MRM acquisition, the amidated and carboxylated forms of the NP may not be resolved if the chromatographic separation between them is insufficient (42).

A similar and newer alternative to MRM is parallel-reaction monitoring (PRM). Unlike MRM, a high-resolution mass analyzer, such as an Orbitrap, is used to detect fragment ions. Quantitation via PRM is similar to MRM, whereby a quantifier *m/z* transition is selected for peak area quantitation; a compelling advantage of PRM is that all fragment ions from the transmitted precursor ions are monitored. Furthermore, the high-resolution analyzer significantly improves measurement confidence because high mass-accuracy fragment ions can be used to confirm the identity of an NP beyond the monitored transitions. Few PRM-based assays have been applied to quantitative NP measurements, though this is a relatively new technique compared to MRM (43, 44). For instance, the Nemes group (45) employed an Orbitrap operating in PRM mode to quantify angiotensin peptides in mouse hypothalami and achieved limits of detection with synthetic standards between 5 amol and 300 zmol (**Figure 1*a***). The mass accuracy and sensitivity of PRM-based quantitation suggest that this technique may become commonplace for targeted NP studies.

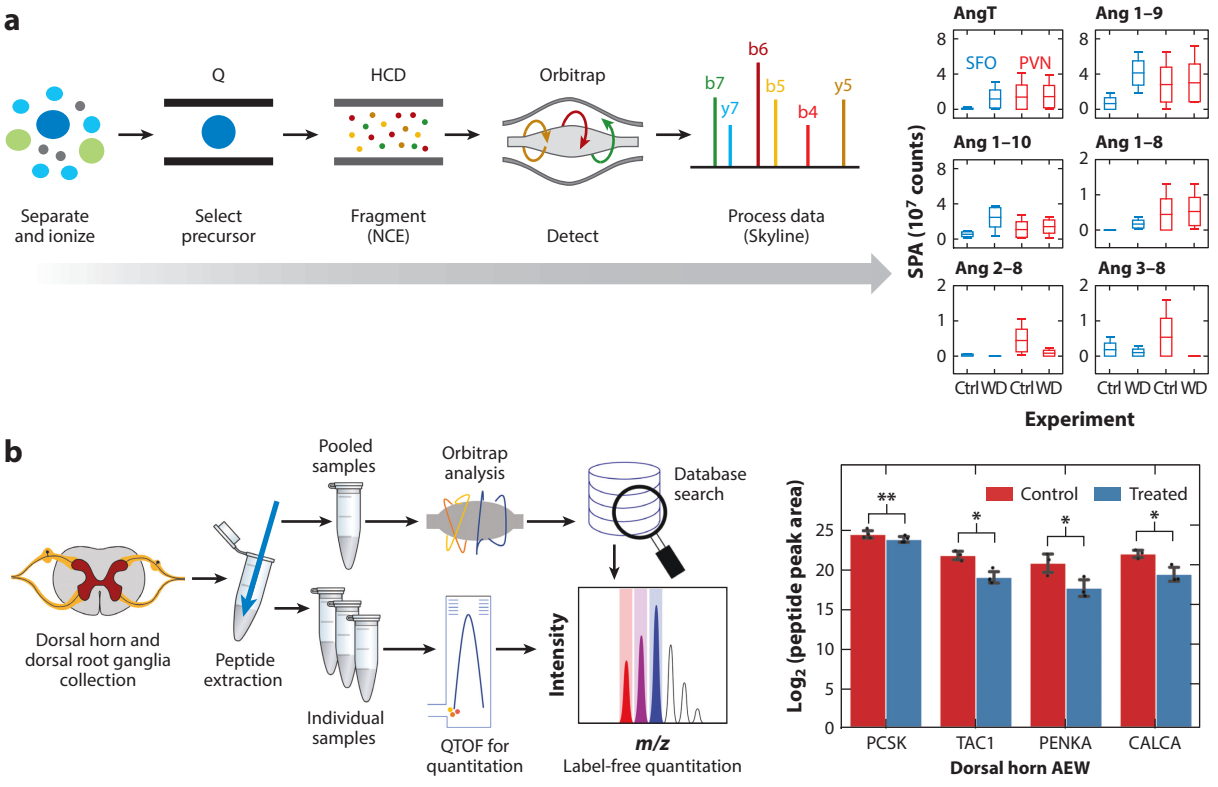

Figure 1

Depiction of targeted and untargeted MS approaches for NP quantitation. (*a*, *left*) Targeted PRM workflow for the quantitation of Ang peptides in the mouse SFO and the PVN. (*a*, *right*) The box-and-whisker plots depict the summed peak areas from the PRM transitions for the selected Ang peptides between control and water-deprived mice in both organs. Panel *a* adapted with permission from Reference 45; copyright 2019 Springer Nature. (*b*) Untargeted LC-MS workflow for the quantitation of NPs from the dorsal horn and dorsal root ganglia of mice. This method employed a dual MS approach where a comprehensive peptide library was first generated from the pooled extracts of either tissue region via LC-MS-Orbitrap analysis, followed by a database search of the obtained MS/MS spectra. The individual samples were separately analyzed via LC-MS-QTOF for MS1 analysis. Label-free quantitation of the peptides was then performed. The bar graph depicts the relative quantitation between various prohormone-derived peptides in the dorsal horn between treated and control samples. Significance values: *, $p < 0.05$; **, $p < 0.01$. Panel *b* adapted with permission from Reference 54; copyright 2020 American Chemical Society. Abbreviations: AEW, acetone/ethyl ether/water; Ang, angiotensin; AngT, angiotensinogen; CALCA, calcitonin gene–related peptide alpha; HCD, higher-energy C-trap dissociation; LC, liquid chromatography; MS, mass spectrometry; MS/MS, tandem mass spectrometry; *m/z*, mass-to-charge ratio; NCE, normalized collision energy; NP, neuropeptide; PCSK, ProSAAS; PENKA, proenkephalin-A; PRM, parallel-reaction monitoring; PVN, paraventricular nucleus; Q, quadrupole; QTOF, quadrupole time-of-flight; SFO, subfornical organ; SPA, summed peak areas; TAC1, protachykinin-1; WD, water-deprived.

The number of NPs that can be quantified in a single MRM or PRM run depends on the number of transitions monitored for each peptide, which in turn may depend on the length of the NP. With longer NPs, more transitions should be monitored for accurate measurements. Monitoring three to five transitions per NP dramatically increases the confidence in assay specificity, although this does reduce throughput. The practical throughput limitations, however, are the cost and availability of the targeted peptide standards for separation optimization and validation of precursor–fragment ion transitions. Scheduling monitored retention times for each transition according to each NP elution window allows dozens of peptides to be measured in a

single analysis. The multiplexed capability of targeted MS approaches yields the most precise quantitation of NPs in neural and neuroendocrine pathways.

Untargeted Mass Spectrometry Quantitation

Unlike targeted approaches where NPs are preselected, untargeted approaches seek to identify and quantify as many NPs in a sample as practical. These measurements are well suited for discovery-oriented research, as they are typically performed in a shotgun manner; novel or unexpected endogenous peptides can be explored under various experimental paradigms. Different workflows for untargeted MS quantitation have been previously reviewed, including labeled or label-free schemes and data-dependent acquisition (DDA) or data-independent acquisition (DIA) (46, 47). This section focuses on highlighting the characteristics and challenges that may be encountered when implementing these approaches specifically for NP quantitation.

Label-Free Versus Labeled Quantitation

One can categorize quantitative approaches based on whether or not they need a label. In label-free quantitative LC-MS measurements, the samples are measured in their native form (no chemical derivatization). Practically, the lack of a chemical label enables the analysis of more biological replicates per sample group, thereby increasing the statistical power of the assays. Although one of the obvious advantages of label-free quantitation is simplified sample preparation, label-free analyses tend to have a lower throughput than labeling schemes; each sample is measured separately, increasing acquisition time and potential variability among samples. Fortunately, various data normalization techniques exist that help minimize these often random biases for more accurate quantitation (48, 49).

Label-free quantitation of NPs typically follows two main approaches: spectral counting and signal comparison via peak area integration. Spectral counting is based on the premise that peptide abundance is proportional to the number of MS2 spectra observed for that peptide (50). While spectral counting-based quantitation is straightforward, factors such as NP structure should be considered in relation to ionization and fragmentation efficiency. For instance, cyclic NPs and large peptide hormones (e.g., oxytocin and insulin) are easily omitted in shotgun MS measurements due to the gas-phase stability imparted by their disulfide bonds, leading to poor fragmentation under typical collision-induced dissociation conditions (51). Different fragmentation techniques have been employed with the goal of obtaining higher-quality MS2 spectra for unusually stable molecules. As one example, to characterize the disulfide bond–containing hyperglycemic hormones in crustacean sinus glands and pericardial organs, Liu et al. (52) employed chemical reduction of disulfide bonds followed by fragmentation with electron-transfer high-energy C-trap dissociation. This approach enabled higher fragmentation efficiency when compared to fragmentation of the NPs using only high-energy collisional C-trap dissociation. Although routinely used in proteomics applications, reduction/alkylation of disulfide bonds is not typically required in peptidomics. This method shows potential for improving MS2 spectral quality for more accurate quantitation of select peptides by spectral counting-based techniques.

Peak area-based quantitation relies on integration of the area under the curve for extracted ion chromatograms (XICs) of each detected peptide. Here, quantitation is performed at the MS1 level and the area of the peptide XIC is compared across replicates (53). This method of untargeted NP quantitation has been employed by various groups to study NP profiles in different physiological models, including migraine, chronic itch, and feeding behavior (26, 54, 55). Tillmaand et al. (54) employed a dual MS-based approach for quantifying NPs in the dorsal horn and dorsal root ganglia of mice in a model of chronic itch. Tissue-specific peptide libraries were

generated by searching Orbitrap-tandem MS (MS/MS) results for pooled tissues against a peptide database. Individual samples were then analyzed by LC-MS-quadrupole time-of-flight (QTOF) to obtain the MS1 spectra for each sample. The resulting MS1 spectra and peptide libraries were then imported into Skyline (56), whereby XIC-based relative quantitation of the peptides was performed (**Figure 1*b***). XIC-based quantitation has been shown to be linearly correlated with peptide abundances, though shifts in chromatographic retention times across samples create the need for peptide retention time alignment and isotopic pattern validation for accurate quantitation.

Quantitation Through Chemical Labeling

Alternatively, if individually labeled peptides in each sample have known, recognizable molecular weight differences, incorporating isobaric or isotopic labels into the peptides allows for multiplexed MS analyses. Multiple chemical labels have been described previously, whereby heavy and light isotopes, or isobaric labels containing unique reporter ions in the MS2 spectrum, are incorporated into the peptides prior to MS analysis to determine the fold-change ratios among the differently labeled isotopic peptides or reporter ions with different masses, respectively (46). For instance, Sauer & Li (57) recently employed custom *N*,*N*-dimethyl leucine isobaric labels to measure the changes in NP profiles in crustacean neuronal tissues in response to copper toxicity. Multiplexing capabilities of up to 21-plex have been reported with this particular isobaric label, but no commercial kit is yet available (58). This multiplexing capability of labeled peptides reduces analysis time but limits the number of biological replicates to the number of distinct labels available. The most parallelized commercial kit currently provides 18-plex labeling capabilities with a proprietary tandem mass tag reagent. Because isobaric labeling approaches work at the MS2 level by comparing the ratios of reporter ions from different tags that are generated upon fragmentation of labeled peptides (46), this feature may limit quantitation to abundant NPs for which high-quality MS/MS can be obtained. Additionally, quantifying NPs with PTMs on N-terminal residues, such as acetylation and pyro-glutamination, may not be possible with isobaric tags that react with primary amines at the N termini of peptides (59).

Data-Dependent Acquisition Versus Data-Independent Acquisition

DDA generates high-quality MS2 spectra, whereby a user-defined subset of the most intense precursor ions from the MS1 survey scan are selected for subsequent MS2 analysis. Through dynamic exclusion of previously sampled precursor ions from MS/MS, DDA workflows facilitate the detection of low-abundance ions that otherwise would not be selected for fragmentation. However, dynamic exclusion may have a detrimental impact on MS2-based quantitation methods, such as spectral counting (60). In contrast, DIA-based quantitation circumvents the semi-stochastic nature of DDA, as all precursor ions from the MS1 survey scan are fragmented using stepwise isolation windows that span the length of the entire *m*/*z* range (61). DIA-based quantitation shows promise for future NP studies, though one of the main difficulties in DIA-based analyses is their dependence on spectral reference libraries, typically generated via DDA methods. Although DDA's high-quality MS2 spectra complement DIA, the compilation of libraries via separate peptidomics analyses increases sample consumption. However, DeLaney & Li (62) recently developed a neuropeptidomic DIA workflow that circumvents the need for a preexisting spectral library by optimizing the *m*/*z* range of the precursor survey scan to reflect the *m*/*z* range encompassing the highest frequency of NPs. This improved DIA method detected over 80 unique NPs, relative to DDA, in both the brain and pericardial organ of *Cancer borealis*, and identified 68 novel putative NPs across both tissue regions. While DDA-based analyses have traditionally been employed for neuropeptidomic quantitative analysis, the high reproducibility and sensitivity of DIA workflows

are promising. They have been reported to increase precision across injections, as evidenced by lower coefficients of variation among technical replicates, to lower the percentages of missing peptide values across samples, increase quantitative accuracy as verified by spike-in experiments, and provide higher numbers of peptide identifications (61–63). Nonetheless, analysis of DIA data remains challenging, with few tools applicable to NPs. Development of user-friendly software packages for interpretation of the complex LC-MS data generated from these experiments may facilitate DIA-based quantitation of neuropeptidomes.

ABSOLUTE QUANTITATION

In contrast to relative quantitation by MS, which compares fold changes between NP profiles, absolute quantitation techniques determine the actual concentration (or amount) of NPs. MS approaches for absolute quantitation must account for analyte physicochemical properties, including isoelectric point, solubility, and conformation, which influence peptide ionization efficiency and signal intensity (64). Structurally different peptides that are equimolar in the sample may produce significantly different signals because of these factors, making absolute quantitation challenging. One technique that accounts for such variabilities and determines absolute NP concentrations is stable isotope dilution. This method compares peak area ratios of a peptide and its isotopically labeled synthetic standard, at various concentrations, to generate a calibration curve. The endogenous peptide concentration can be extrapolated by spiking a known amount of the isotope standard into the sample (53). This approach, combined with MRM measurements, has been used for quantifying endogenous neuropeptides in various tissues and fluids. For instance, Hopkins et al. (65) developed an LC-MS assay employing stable isotope dilution in conjunction with MRM to quantify orexin A in the cerebrospinal fluid of a mouse model of sleep deprivation. The assay achieved an impressive limit of quantitation of 1.65 fM, with intra- and interday variabilities of less than 10%. Endogenous concentrations of orexin A in the cerebrospinal fluid were determined to range from 660 to 3,500 amol/μL. Although this approach is simple, it is expensive and has limited throughput because custom isotopically labeled standards are required for each peptide of interest. Assay validation must be optimized as well, accounting for linearity across concentration ranges and matrix effects from tissue samples.

Absolute quantitation is less common for neurochemical investigation because a typical study design looks for induced NP changes relative to physiologically normal controls. Such changes can be captured with relative quantitation at lower costs and with fewer resources while probing a broader subset of NPs for more in-depth insights into molecular signaling events.

ION MOBILITY SPECTROMETRY

The hyphenated analytical approaches described above serve as effective analysis tools for structural and quantitative characterization of complex endogenous peptides samples; however, throughput and linear dynamic range for quantitation need improvement for some applications. One solution for increasing the depth of peptidome coverage and quantitation accuracy is integrating IMS measurements as an additional separation dimension between the liquid separation and the mass analyzer. In IMS, gas-phase ions of different shapes travel with different velocities in a weak electric field of a drift cell filled with a buffer gas—in essence, this is a gas-phase form of electrophoresis that separates ions according to their gas-phase molecular shapes (66). LC-IMS-MS can offer increased ion utilization efficiency, improved sensitivity and specificity of detection, and broader dynamic range. Because of the introduction of a new range of IMS instruments, this approach is rapidly gaining application in traditional proteomics analysis (67), including quantitation (68), and is advantageous for NPs (69–72).

LC-IMS-MS evaluates samples based on four distinct dimensions (retention time, drift time, *m/z*, and intensity) and increases the number of peptide precursor ions that are targeted for sequencing in a single acquisition. This results in a dramatic increase of peptide identification rates and specificity of detection, even in samples of high anatomical and chemical complexity. Importantly, confident identifications are possible from chimeric tandem spectra of multiple coeluted peptides with different ion mobilities. IMS reduces the burden of sample preparation by eliminating previously essential prefractionation steps prior to LC-MS. Fewer steps and less handling during sampling open opportunities for analysis of mass-/volume-limited samples, including single cells (73).

Several commercial, conceptually different instruments with ion mobility capabilities have recently been released on the market: field asymmetric IMS (FAIMS) (74), traveling wave (75), and trapped ion mobility spectrometry (TIMS). Due to space limitations, we focus our discussion on the increased sensitivity provided by TIMS analysis (76).

Nested LC-IMS-MS measurements are effectively lossless in terms of the peptide ion signals due to the ability to concentrate ions before the IMS step and reduce the background from the IMS separation. In one embodiment, parallel accumulation serial fragmentation (PASEF) enables large enhancements in detectability/sensitivity in a high-throughput manner for complex samples. This technology is available with both electrospray ionization (ESI) and matrix-assisted laser desorption/ionization (MALDI) configurations, making IMS directly accessible for both liquid samples and analyzing single cells with high spatial resolution (77). By synchronizing precursor selection with gas-phase TIMS separation, one can select up to 120 precursor ions within a single ion mobility scan, increasing sequencing speed severalfold without losses in sensitivity. This strategy of ion accumulation and analysis provides improvements to high-throughput MS2 analysis and sensitivity, enabling small-volume, mass-limited studies in a quantitative manner (78). In a typical DDA scheme combined with PASEF, MS2 precursor selection is dynamic and based on *m/z* signal intensity and ion mobility. The DIA-PASEF mode concurrently fragments numerous precursors within relatively broad, user-defined *m/z* ranges. In contrast to traditional DIA or SWATH-MS (sequential window acquisition of all theoretical spectra mass spectroscopy) workflows, where wide isolation windows result in noisy fragment ion spectra, DIA-PASEF is more sensitive and selective.

With all IMS measurements, the inclusion of the peptide collisional cross sections (derived from the ion mobility separation) facilitates differentiation of isobaric sequences or positional isomers of PTMs, thereby extending the analytical possibilities for NPs to conformational analysis for improved compound identification, to confident library matching, and potentially, to lower FDRs in large data sets (52, 69). One notable example of a challenging PTM is isomerization of a single amino acid in a peptide from the L to D conformation. D-Amino acid–containing peptides (DAACPs) are notorious for being difficult to characterize by MS because isomerization does not change the molecular mass of the peptide (79). Recently though, a CE-IMS workflow (**Figure 2*a***) was developed in which analysis of a DAACP NP in single neurons and connective tissues revealed numerous stereoisomers (80) (**Figure 2*b–g***). For relative quantitation of the NP diastereomers across these samples, the peak areas of native NP mobility profiles were compared to a simulated calibration curve based on synthetic NP mobility profiles. By comparing relative abundances of NPs throughout the nervous system, it may be possible to determine where unusual PTMs occur.

Currently, interpretation of raw IMS data inflated by the addition of the fourth dimension, and easily reaching 10 GB per sample, poses a computational challenge. While instrument vendors quickly introduced real-time data reduction strategies resulting in file sizes of ~1 GB, typical for LC-MS/MS, the data architecture is not readily compatible with existing bioinformatics. Our impression is that the advancement of bioinformatics resources for IMS-MS/MS raw data analysis

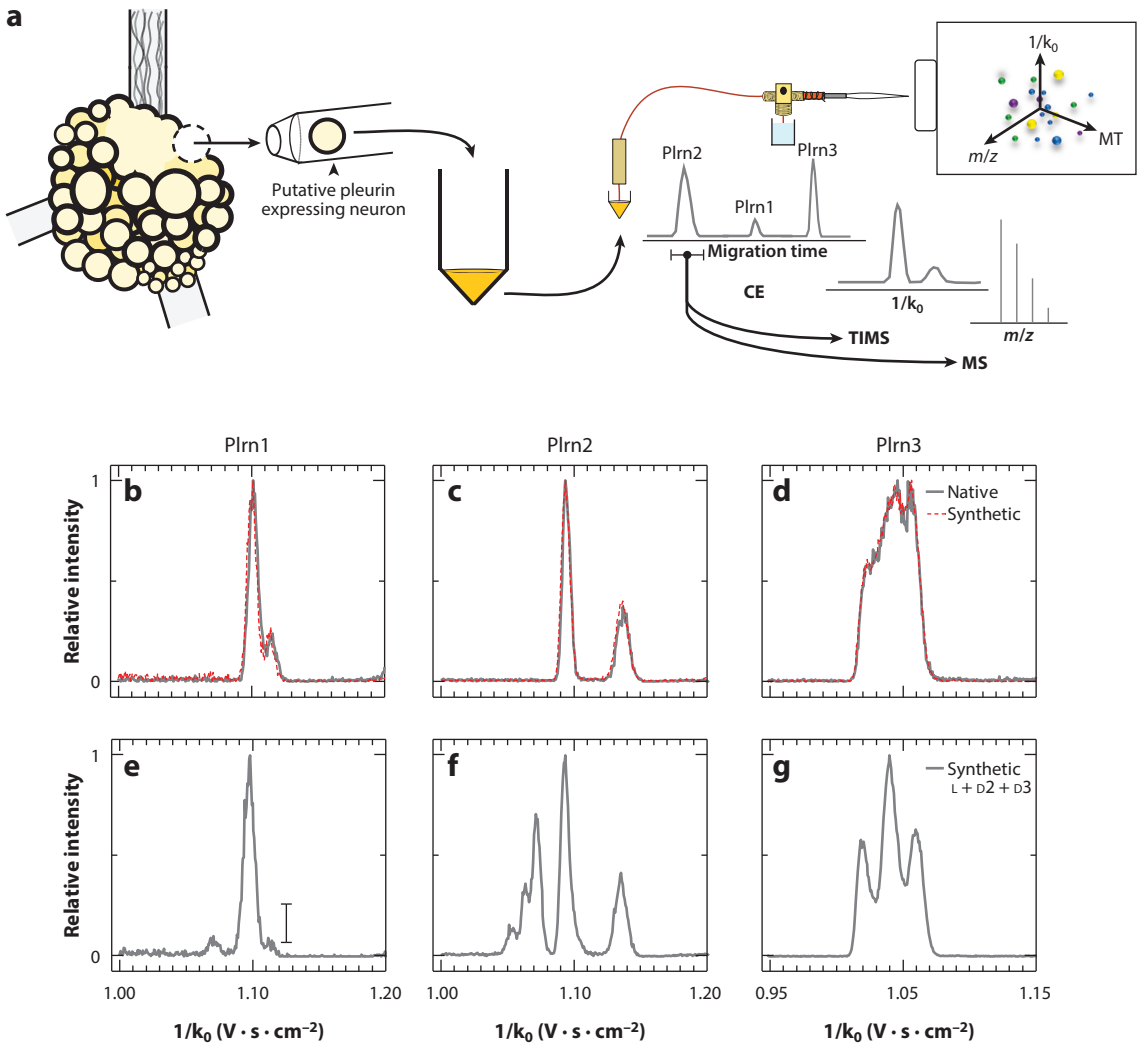

Figure 2

Analysis of individual neurons by CE-nanoESI-TIMS-TOF MS. (*a*) The workflow includes single-cell sampling, neuropeptide extraction, CE separation, and MS measurements on a TIMS-TOF instrument that result in three-dimensional data: CE MT, *m/z*, and reduced ion mobility ($1/k_0$). Using this approach, stereochemical configurations of three neuropeptides, Plrn1, Plrn2, and Plrn3, derived from the pleurin precursor in individual neurons in the central nervous system of *Aplysia californica*, were determined by comparison of the mobility profiles of synthetic and native Plrn1–Plrn3 peptides. (*b–d*) Assignment of native Plrn1–Plrn3 stereochemistry in the pleurin neuron by TIMS. Plots show overlaid EIMs of native (*b*) Plrn1, (*c*) Plrn2, and (*d*) Plrn3 with the corresponding synthetic ^{13}C-labeled all-L standard. (*e–g*) EIMs of 1:1:1 mixtures of synthetic ^{13}C-labeled L-, D2-, D3- (*e*) Plrn1, (*f*) Plrn2, and (*g*) Plrn3. The vertical bar in panel *e* highlights the differences between the mobility fingerprints of the pure L-Plrn1 in panel *b* and the combined L-, D2-, and D3-Plrn1 shown in panel *g*. EIMs in panels *b–g* are of the $[m+2H]^{2+}$ or $[m^*+2H]^{2+}$ ions. Abbreviations: CE, capillary electrophoresis; EIM, extracted ion mobilogram; ESI, electrospray ionization; MS, mass spectrometry; MT, migration time; *m/z*, mass-to-charge ratio; TIMS, trapped ion mobility spectrometry; TOF, time-of-flight. Figure adapted with permission from Reference 80; copyright 2021 American Chemical Society.

lags behind rapidly progressing MS instrumentation. Although all major MS vendors offer some form of IMS on their flagship instruments, few bioinformatics tools are currently capable of effective processing of multidimensional data (81, 82). Quantitation of endogenous peptides whose levels are assessed irrespective of other peptides matching the same precursor protein is especially limited at this time, which hinders implementation of this technology in direct quantitation of NPs on the global scale.

MASS SPECTROMETRY IMAGING

With the introduction of MSI for large molecules in biological samples ~20 years ago, it is possible to visualize the spatial localization of NPs within tissues (83). Briefly, MSI is usually performed by creating a two-dimensional (2D) sampling grid across the surface of the tissue; mass spectra are then collected at each point along the grid. The resulting data can be translated into a heat map representing the abundance of selected ions across the tissue surface. The soft ionization provided by MALDI makes it a practical choice for producing easily interpretable spectra of singly charged, intact peptides and proteins. Alternatives to MALDI (84, 85) and ambient ionization (86, 87) techniques are available for imaging but are generally more suitable for small molecules and lipids. Comparing MS images of tissues from different models, e.g., behavioral, disease, or therapeutic, allows correlation of NP signals and tissue structures that can reveal NP signaling or transport mechanisms during normal or perturbed functioning. For accurate and sensitive measurements of NPs by MSI, optimization of parameters for relative quantitation of neuropeptide distributions such as tissue preparation, spatial resolution, and instrumentation is vital.

NPs are stored within dense core vesicles in tissues. Efficient extraction of NPs and removal of interfering matrices are important for obtaining the reproducible signals required for comparing the abundance of NPs under different biological conditions. Many established tissue washes were not designed with the goal of NP detection, but rather protein detection. In the past ~7 years, a variety of organic solvent–based tissue washes (88–91) have been developed, with an emphasis on solvent choice and strict monitoring of timing for removal of biological salts while preserving NP localization (88, 92, 93). Furthermore, advanced derivatization techniques have been developed to remove interfering matrices from NPs. As one example, the use of nanosecond photochemical reaction (nsPCR) click chemistry induces thermo- and electrophoretic separation of cationic salts and matrices from NPs directly on the tissue (**Figure 3*a***), preserving spatial information and enhancing NP detection (94). Further improvement of the nsPCR labeling efficiency may provide a more general technique for on-tissue quantitation. In addition to fresh and frozen tissue, MSI can be extended to fixed tissues from clinically relevant samples. The development of a digestion-free deparaffination method facilitated NP detection in fixed tissues up to 30 years old (95). Although improving extraction of NPs from tissues is of great interest, these efforts must be balanced with efforts to maintain their spatial localization.

As the foremost goal of MSI is to provide information about the spatial localization of NPs within a tissue section, recent advancements have aimed to improve the spatial resolution of the imaging techniques. Laser spot diameter, step size, and the matrix application are user-controlled parameters that directly affect the obtainable lateral resolution. Furthermore, both the matrix-solvent and crystallization rates will affect what types of peptides are seen in MALDI analyses (96). With the development of automated matrix applicators, it is easier to balance extraction efficiency and delocalization (88). Further improvements provide near-single-cell spatial resolution of 25 μm and below by utilizing finely focused lasers and small step sizes (43, 90, 95, 97, 99) or using alternative ionization sources such as primary ion beams (100). Spatial resolution has even reached the subcellular level, nearing 1 μm (101, 102). These advances enable visualization of finer structural-chemical details within tissues.

Two key factors limit obtaining enhanced spatial localization, even when the instrument is capable of it. First, as the spot size decreases, the area of tissue sampled is reduced as the square of the reduction; reducing the spot size dramatically decreases the available material to measure. In addition, more spots need to be assayed per tissue area, increasing the analysis time and its effect on sample integrity and throughput. Better spatial resolution correlates with more time under vacuum during which the MALDI matrix can sublime from the tissue. In some cases, sampling time can

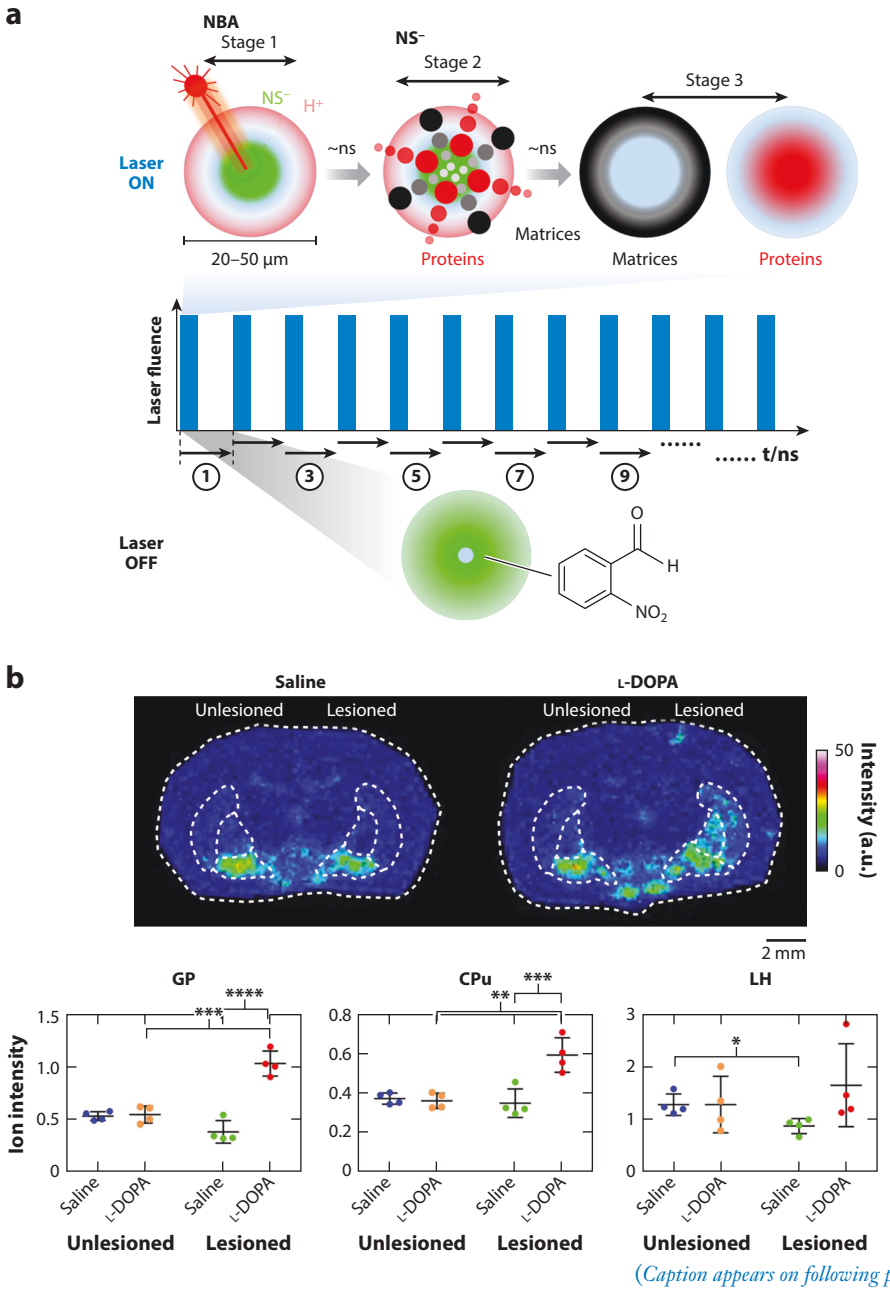

(Caption appears on following page)

Figure 3 (*Figure appears on preceding page*)

Highlighted mass spectrometry imaging (MSI) techniques for tissue treatment and relative quantitation. (*a*) Tissue treatment by nanosecond photochemically promoted click chemistry for on-tissue separation of peptides and matrices controlled by the matrix-assisted laser desorption/ionization (MALDI) laser on/off switch. In stages 1–3, laser excitation of 2-nitrobenzaldehyde (NBA) labels peptides and proteins to establish a microelectric field thermal gradient, peptides and proteins then separate from matrices, and finally peptides/proteins are concentrated to the center of the 20–50-μm laser spot. This process provides up to 93% labeling efficiency and shows promise as an on-tissue, labeled quantitation technique. Panel *a* adapted with permission from Reference 94 (CC BY 4.0). (*b*) MALDI-MSI was used to visualize neuropeptide alterations in a Parkinson's disease model displaying four different treatments: unlesioned, lesioned, saline, and L-3, 4-dihydroxyphenylalanine (L-DOPA). Results for dynorphin-B are shown here. For relative quantitation, both a two-way ANOVA and a posthoc Sidak's multiple comparison test were used to determine significant differences in neuropeptide abundance across three brain regions: globus pallidus (GP), caudate-putamen (CPu), and lateral hypothalamus (LH). Significance values: *, $p \leq 0.05$; **, $p \leq 0.01$; ***, $p \leq 0.001$; ****, $p \leq 0.0001$. Panel *b* adapted with permission from Reference 89; copyright 2020 Elsevier.

be decreased from days to hours by increasing stage movement speed (101, 102). Additionally, atmospheric pressure (AP)-MALDI can be used to eliminate the effects of vacuum on sample integrity while maintaining spectral resolution (102, 103). Recently, Li et al. (103) developed a sub-AP-MALDI source through optimization of intermediate pressure conditions, alleviating ion suppression effects seen in traditional AP sources and improving the sensitivity of simultaneous imaging of NPs and lipids in mouse brain tissue.

MSI is commonly used to compare the effects of stressors (88, 104), behaviors (90), and disease processes (89, 92, 105, 106) on the abundance of NPs. Due to the variability in ionization, most quantitation in MSI is done using relative measures of ion abundance both within and across tissues. Within tissues it is useful to determine changes in NP localization across different structures, for example, to investigate signaling mechanisms (107). Cross-tissue comparisons also provide NP signaling information with regard to inducing different behaviors (90) or disease therapies (89). To determine whether the differences in NP signals are significant or occur due to variability in ionization or sampling artifacts, a variety of statistical tests are used (89, 95, 106). For example, multivariate data analysis on NPs in Parkinson's disease models (**Figure 3*b***) revealed significant differences in NP abundances and previously unreported NP regulation in areas of the brain critical to locomotion (89). Relative quantitation of NP abundance and distribution provides valuable insight into the chemical consequences of various conditions.

Peptides in tissue extracts can also be quantified using imaging platforms. These techniques discard spatial information for improved quantitation for MALDI-MSI analysis of NPs across biological conditions (104, 107). The quantified tissue extracts can be directly compared to tissue images because the same ion source is used for both data sets. This comparison is useful because some NPs show changes in localization but not concentration or vice versa, while other NPs show changes in both parameters (107).

Furthermore, MALDI-MSI peptide detection can be improved by coupling separation methods. DeLaney & Li (108) demonstrated that the number of NPs detected can be significantly increased by depositing a continuous trace of CE-separated NPs on a MALDI substrate. Development of these hyphenated techniques provides a complementary analysis of NPs compared to classical separations, as different ionization techniques excite different NPs. Additionally, the abundance and localization of lipids (43) and neurotransmitters (109, 110) can be obtained simultaneously to provide context about NP functions. The resulting MS images can be compared to immunostaining of analogous or the same tissue sections post-MALDI for comparison of chemical and anatomical structures, respectively (92, 95, 98, 105). The combination of imaging modalities can reveal the interplay between different structural and chemical patterns within tissues.

SINGLE-CELL MASS SPECTROMETRY

Although MSI reveals the spatial location of NPs within tissues, the resulting NP profiles are generally averaged over many cells. Even with MSI spatial resolution reaching the dimension of the cell body, mechanical sectioning of tissues and the intertwining of cellular projections throughout tissues cause overlap of individual cell signals. To probe the cellular heterogeneity of these tissues, single cells can be isolated and analyzed individually. While the specific spatial location of NPs is lost, chemical heterogeneity and detection of rare cellular populations, or low-abundance NPs, are gained. Similarly, single-cell molecular techniques, such as polymerase chain reaction and RNA-sequencing, allow an understanding of the heterogeneity of gene expression (111). Single-cell MS excels as a complementary technique to transcriptomics, as it provides untargeted detection of the NP gene products (112). Methods utilizing strategies to explore and quantitate the heterogeneity of cellular populations are discussed below.

High-Throughput Single-Cell Classification

Developments in single-cell sampling and analysis have advanced high-throughput detection capabilities for classification of cellular populations by MS (113). MALDI-MS is well suited for analysis of small volumes because it requires few sample preparation steps, thereby reducing sample loss. For analysis of single cells by MALDI, cells must be isolated from tissues and deposited on a MALDI-compatible substrate. Single cells may be surgically dissected from tissue (114–116) or enzymatically dissociated (117–120). Enzymatic dissociation can produce thousands of cells suitable for analysis; however, we find that dissociation protocols must be optimized for specific cell types and animal models to guarantee the structural and chemical integrity of the cell. To enable characterization of thousands of cells, optical images of dispersed isolated cells may be used to align the MALDI laser with single cells on the sample holder (121). Sensitivity, robustness, and scan rates up to 2 kHz make MALDI compatible with high-throughput analysis of thousands of single cells. In combination with a TOF analyzer, sampling times of ~1 s/cell with large m/z range capabilities can be achieved (117–119). The combination of MALDI with a Fourier transform ion cyclotron resonance analyzer leads to increased spectra acquisition time but dramatically increases mass resolution relative to MALDI-TOF (122).

Though the information gained from each cell is less than that from a larger, homogenized sample, a compelling advantage of profiling thousands of individual cells per sample is the increased power of statistical tests for categorization of cellular populations. Statistical analysis of spectral characteristics from individual cells by principal component analysis (117–119), clustering techniques (117, 118), and machine learning (123) allows the cells' chemical heterogeneity to be categorized and quantified for comparison to known cell identities. These methods allow identification of rare cells and subpopulations that would be undetected in bulk measurements (117). Understanding this variation is important, as a single neuron can be responsible for certain physiological functions (124).

Furthermore, because MALDI leaves behind a majority of the sample (125), individual cells can be probed multiple times by MALDI (117) or complementary methods for testing different hypotheses. Multi-omics measurements have become possible through other ionization sources for complimentary metabolomic or lipidomic measurements of the same cells (126, 127). After classification of cells by their NP profiles, Comi et al. (127) utilized liquid microjunction extraction on the same cells for low-mass metabolite detection by CE-ESI-MS. Accordingly, this multiplexed method profiled a broader range of chemical species while reducing spectral complexity and ion suppression effects by capitalizing on the advantages of each technique. Through

multi-omics, single-cell measurements provide clues about NP function in cell–cell signaling processes.

Subcellular Mass Spectrometry

As part of the secretory process, newly synthesized NPs are sorted into secretory granules, where they are concentrated and stored, awaiting release stimuli. Importantly, NP sorting and packaging influence the physiological actions of peptides. Singular NPs located to the same vesicle are obligatory cotransmitters. However, if sorted into distinct granules, their release and function can be regulated independently within the same cell (128, 129). Therefore, chemical profiling of secretory granules and other subcellular structures presents significant interest. A surprising advantage of subcellular MS is the reduction of overall sample complexity and access to high, local concentrations of NPs.

Subcellular MS via secondary ionization mass spectrometry (SIMS) is highly amenable for metabolomics (130, 131); however, SIMS is not ideal for the analysis of most NPs due to significant fragmentation of their larger molecular ions. To avoid NP fragmentation, bulk (132) or single-organelle (73, 133) measurements are accessible by ESI-MS or MALDI-MS. In 2000, Rubakhin et al. (133) devised a micromanipulator-controlled micropipette to collect single dense core vesicles for MALDI-MS profiling of NPs in volumes >300 aL; this technique was expanded recently to measuring hundreds of individual dense core vesicles to distinguish several classes of vesicles (134). Microsampling techniques (135) can also be adapted to extract NP contents directly from subcellular compartments, such as the nucleus and cytoplasm (73). In all cases, sample preparation is important for reducing NP delocalization (136). Further development of high-throughput organelle isolation would provide a valuable opportunity for optically guided, subcellular MALDI-MS.

Single-Cell Quantitation

There are a variety of approaches for single-cell quantitation, as highlighted in **Figure 4**. However, NP quantitation in single cells faces many challenges. Foremost, compared to single-cell transcriptomics approaches, there are no amplification techniques available for NPs. Labeled quantitation (135, 137) is possible; however, incomplete labeling of NP species may result in a loss of signal due to smaller NP copy numbers in single cells versus bulk samples. For label-free quantitation, a variety of statistical techniques are well suited for relative quantitation across samples. In subcellular MS, multivariate statistical analysis of normalized NP signals has revealed distinct differences in NP abundances across cellular compartments, providing clues about NP transport, creation, and degradation (73). Alternatively, calibration curves may be simulated from NP mobility profiles, benefiting from the additional separation afforded by IMS (80). Clearly, this area would benefit from one standardized, user-friendly technique to obtain quantitative results from single cells.

LOOKING AHEAD

This review highlights the current status of NP measurements with MS, including a range of approaches for quantitation, localization, and single-cell measurements. With the introduction of enhanced IMS instruments and newer protocols for single-cell analyses, the future of NP characterization is exciting. The time and effort required for more routine studies are decreasing, more standardized approaches are available, and the ability to interweave NP data and transcriptomics, and perhaps LC-MS-based quantitation with MSI and single-cell studies, all point to the ability to gain improved information on NPs from a broader range of tissues.

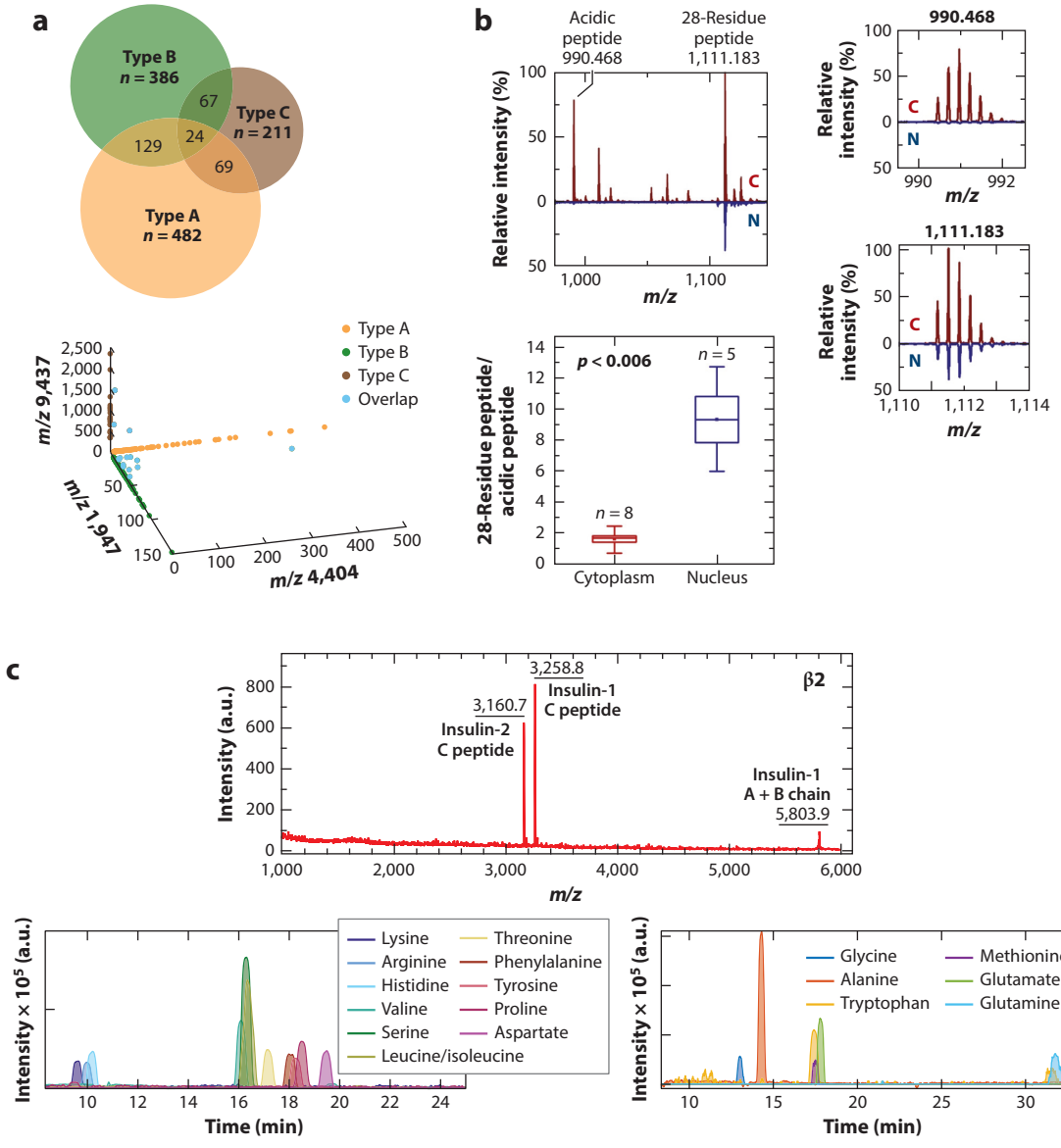

Figure 4

Highlighted single-cell MS methods for categorization, relative quantitation, and multi-omics measurements of cellular populations. (*a*) Results of hierarchical clustering of neuropeptide profiles for categorization of thousands of dorsal root ganglia cells. (*Top*) The Venn diagram represents the three primary cellular populations labeled Type A, B, and C. (*Bottom*) Individual cells are plotted with respect to the presence of selected neuropeptide markers indicative of each type: *m/z* 9,437 (Type C), *m/z* 1,947 (Type B), and *m/z* 4,404 (Type A). Panel *a* adapted with permission from Reference 117; copyright 2018 Wiley-VCH. (*b*, *top*) Comparison of mass spectra from the cytoplasm (C) and nucleus (N) illustrating the differences in abundance of two selected neuropeptides: acidic peptide (+4, *m/z* 990.468) and a previously unreported 28-residue peptide (+3, *m/z* 1,111.183). (*b*, *bottom*) The box-and-whisker plot demonstrates a significantly lower abundance of acidic peptide in the nucleus than the cytoplasm. Panel *b* adapted from Reference 73 (CC BY 4.0). (*c*) Interfacing of MALDI-MS for high-throughput detection of neuropeptides followed by CE-ESI-MS for in-depth profiling of small metabolites from an individual pancreatic islet cell. This method was utilized to discriminate between α and β cell types. The MALDI mass spectrum and two electropherograms shown are representative of a β2 cell. Panel *c* adapted with permission from Reference 127; copyright 2017 American Chemical Society. Abbreviations: CE, capillary electrophoresis; ESI, electrospray ionization; MALDI, matrix-assisted laser desorption/ionization; MS, mass spectrometry; *m/z*, mass-to-charge ratio.

DISCLOSURE STATEMENT

The authors are not aware of any affiliations, memberships, funding, or financial holdings that might be perceived as affecting the objectivity of this review.

ACKNOWLEDGMENTS

The authors acknowledge support under award number P30 DA018310 from the National Institute on Drug Abuse. S.E.B. was supported by the National Science Foundation under grant 1735252. The content is solely the responsibility of the authors and does not necessarily represent the official views of the US National Institutes of Health.

LITERATURE CITED

1. Burbach JPH. 2011. What are neuropeptides? In *Neuropeptides: Methods and Protocols*, ed. A Merighi, pp. 1–36. Totowa, NJ: Humana Press
2. Meriney SD, Fanselow EE. 2019. Neuropeptide transmitters. In *Synaptic Transmission*, ed. SD Meriney, EE Fanselow, pp. 421–34. Amsterdam: Academic
3. Navratilova E, Porreca F. 2019. Substance P and inflammatory pain: getting it wrong and right simultaneously. *Neuron* 101(3):353–55
4. Wang C, Wang Q, Ji B, Pan Y, Xu C, et al. 2018. The orexin/receptor system: molecular mechanism and therapeutic potential for neurological diseases. *Front. Mol. Neurosci.* 11:220
5. Garrahy A, Thompson CJ. 2019. Vasopressin. In *Encyclopedia of Endocrine Diseases*, ed. I Huhtaniemi, L Martini, pp. 29–35. Oxford, UK: Academic. 2nd ed.
6. van der Klaauw AA. 2018. Neuropeptides in obesity and metabolic disease. *Clin. Chem.* 64(1):173–82
7. Sah R, Geracioti TD. 2013. Neuropeptide Y and posttraumatic stress disorder. *Mol. Psychiatry* 18(6):646–55
8. Mendel HC, Kaas Q, Muttenthaler M. 2020. Neuropeptide signalling systems—an underexplored target for venom drug discovery. *Biochem. Pharmacol.* 181:114129
9. DeLaney K, Sauer CS, Vu NQ, Li L. 2018. Recent advances and new perspectives in capillary electrophoresis-mass spectrometry for single cell "omics." *Molecules* 24(1):42
10. Abid MSR, Mousavi S, Checco JW. 2021. Identifying receptors for neuropeptides and peptide hormones: challenges and recent progress. *ACS Chem. Biol.* 16(2):251–63
11. Bowman AP, Blakney GT, Hendrickson CL, Ellis SR, Heeren RMA, Smith DF. 2020. Ultra-high mass resolving power, mass accuracy, and dynamic range MALDI mass spectrometry imaging by 21-T FT-ICR MS. *Anal. Chem.* 92(4):3133–42
12. May JC, McLean JA. 2016. Advanced multidimensional separations in mass spectrometry: navigating the big data deluge. *Annu. Rev. Anal. Chem.* 9:387–409
13. Vu NQ, DeLaney K, Li L. 2021. Neuropeptidomics: improvements in mass spectrometry imaging analysis and recent advancements. *Curr. Protein Pept. Sci.* 22(2):158–69
14. Timp W, Timp G. 2020. Beyond mass spectrometry, the next step in proteomics. *Sci. Adv.* 6(2):eaax8978
15. Ridgeway ME, Lubeck M, Jordens J, Mann M, Park MA. 2018. Trapped ion mobility spectrometry: a short review. *Int. J. Mass Spectrom.* 425:22–35
16. Hui K-S. 2007. Neuropeptidases. In *Handbook of Neurochemistry and Molecular Neurobiology: Neural Protein Metabolism and Function*, ed. A Lajtha, pp. 625–51. New York: Springer
17. Fridjonsdottir E, Nilsson A, Wadensten H, Andrén PE. 2018. Brain tissue sample stabilization and extraction strategies for neuropeptidomics. In *Peptidomics: Methods and Strategies*, ed. M Schrader, L Fricker, pp. 41–49. New York: Springer
18. O'Callaghan JP, Sriram K. 2004. Focused microwave irradiation of the brain preserves in vivo protein phosphorylation: comparison with other methods of sacrifice and analysis of multiple phosphoproteins. *J. Neurosci. Methods* 135(1):159–68
19. Secher A, Kelstrup CD, Conde-Frieboes KW, Pyke C, Raun K, et al. 2016. Analytic framework for peptidomics applied to large-scale neuropeptide identification. *Nat. Commun.* 7:11436

20. Yang N, Anapindi KDB, Romanova EV, Rubakhin SS, Sweedler JV. 2017. Improved identification and quantitation of mature endogenous peptides in the rodent hypothalamus using a rapid conductive sample heating system. *Analyst* 142(23):4476–85
21. Keller D, Erö C, Markram H. 2018. Cell densities in the mouse brain: a systematic review. *Front. Neuroanat.* 12:83
22. Russo AF. 2017. Overview of neuropeptides: Awakening the senses? *Headache* 57(Suppl. 2):37–46
23. Reubi JC. 1995. Neuropeptide receptors in health and disease: the molecular basis for in vivo imaging. *J. Nucl. Med.* 36(10):1825–35
24. Ediage EN, Aerts T, Lubin A, Cuyckens F, Dillen L, Verhaeghe T. 2019. Strategies and analytical workflows to extend the dynamic range in quantitative LC-MS/MS analysis. *Bioanalysis* 11(12):1189–1206
25. Hohenester UM, Barbier Saint-Hilaire P, Fenaille F, Cole RB. 2020. Investigation of space charge effects and ion trapping capacity on direct introduction ultra-high-resolution mass spectrometry workflows for metabolomics. *J. Mass Spectrom.* 55(10):e4613
26. Anapindi KDB, Yang N, Romanova EV, Rubakhin SS, Tipton A, et al. 2019. PACAP and other neuropeptide targets link chronic migraine and opioid-induced hyperalgesia in mouse models. *Mol. Cell. Proteom.* 18(12):2447–58
27. Unsihuay D, Sanchez DM, Laskin J. 2021. Quantitative mass spectrometry imaging of biological systems. *Annu. Rev. Phys. Chem.* 72:307–29
28. Cox J, Hein MY, Luber CA, Paron I, Nagaraj N, Mann M. 2014. Accurate proteome-wide label-free quantification by delayed normalization and maximal peptide ratio extraction, termed MaxLFQ. *Mol. Cell. Proteom.* 13(9):2513–26
29. Chen C, Hou J, Tanner JJ, Cheng J. 2020. Bioinformatics methods for mass spectrometry-based proteomics data analysis. *Int. J. Mol. Sci.* 21(8):2873
30. Harno E, Gali Ramamoorthy T, Coll AP, White A. 2018. POMC: the physiological power of hormone processing. *Physiol. Rev.* 98(4):2381–2430
31. Moritz CP, Mühlhaus T, Tenzer S, Schulenborg T, Friauf E. 2019. Poor transcript-protein correlation in the brain: negatively correlating gene products reveal neuronal polarity as a potential cause. *J. Neurochem.* 149(5):582–604
32. Webb-Robertson BJM, Wiberg HK, Matzke MM, Brown JN, Wang J, et al. 2015. Review, evaluation, and discussion of the challenges of missing value imputation for mass spectrometry-based label-free global proteomics. *J. Proteome Res.* 14(5):1993–2001
33. Song M, Greenbaum J, Luttrell J, Zhou W, Wu C, et al. 2020. A review of integrative imputation for multi-omics datasets. *Front Genet.* 11:570255
34. Lazar C, Gatto L, Ferro M, Bruley C, Burger T. 2016. Accounting for the multiple natures of missing values in label-free quantitative proteomics data sets to compare imputation strategies. *J. Proteome Res.* 15(4):1116–25
35. Bramer LM, Irvahn J, Piehowski PD, Rodland KD, Webb-Robertson B-JM. 2021. A review of imputation strategies for isobaric labeling-based shotgun proteomics. *J. Proteome Res.* 20(1):1–13
36. Pascovici D, Handler DC, Wu JX, Haynes PA. 2016. Multiple testing corrections in quantitative proteomics: a useful but blunt tool. *Proteomics* 16(18):2448–53
37. Korthauer K, Kimes PK, Duvallet C, Reyes A, Subramanian A, et al. 2019. A practical guide to methods controlling false discoveries in computational biology. *Genome Biol.* 20(1):118
38. Saidi M, Beaudry F. 2015. Liquid chromatography-electrospray linear ion trap mass spectrometry analysis of targeted neuropeptides in Tac1$^{-/-}$ mouse spinal cords reveals significant lower concentration of opioid peptides. *Neuropeptides* 52:79–87
39. Mast DH, Checco JW, Sweedler JV. 2020. Differential post-translational amino acid isomerization found among neuropeptides in *Aplysia californica*. *ACS Chem. Biol.* 15(1):272–81
40. Mani DR, Abbatiello SE, Carr SA. 2012. Statistical characterization of multiple-reaction monitoring mass spectrometry (MRM-MS) assays for quantitative proteomics. *BMC Bioinform.* 13(16):S9
41. Kaklamanos G, Aprea E, Theodoridis G. 2020. Mass spectrometry: principles and instrumentation. In *Chemical Analysis of Food*, ed. Y Pico, pp. 525–52. London: Academic. 2nd ed.
42. Virág D, Dalmadi-Kiss B, Vékey K, Drahos L, Klebovich I, et al. 2020. Current trends in the analysis of post-translational modifications. *Chromatographia* 83(1):1–10

43. Chen B, OuYang C, Tian Z, Xu M, Li L. 2018. A high resolution atmospheric pressure matrix-assisted laser desorption/ionization-quadrupole-Orbitrap MS platform enables in situ analysis of biomolecules by multi-mode ionization and acquisition. *Anal. Chim. Acta* 1007:16–25
44. Saidi M, Kamali S, Beaudry F. 2019. Neuropeptidomics: comparison of parallel reaction monitoring and data-independent acquisition for the analysis of neuropeptides using high-resolution mass spectrometry. *Biomed. Chromatogr.* 33(7):e4523
45. Lombard-Banek C, Yu Z, Swiercz AP, Marvar PJ, Nemes P. 2019. A microanalytical capillary electrophoresis mass spectrometry assay for quantifying angiotensin peptides in the brain. *Anal. Bioanal. Chem.* 411(19):4661–71
46. Bąchor R, Waliczek M, Stefanowicz P, Szewczuk Z. 2019. Trends in the design of new isobaric labeling reagents for quantitative proteomics. *Molecules* 24(4):701
47. Krasny L, Huang PH. 2021. Data-independent acquisition mass spectrometry (DIA-MS) for proteomic applications in oncology. *Mol. Omics* 17(1):29–42
48. Willforss J, Chawade A, Levander F. 2019. NormalyzerDE: online tool for improved normalization of omics expression data and high-sensitivity differential expression analysis. *J. Proteome Res.* 18(2):732–40
49. Välikangas T, Suomi T, Elo LL. 2018. A systematic evaluation of normalization methods in quantitative label-free proteomics. *Brief. Bioinform.* 19(1):1–11
50. Rozanova S, Barkovits K, Nikolov M, Schmidt C, Urlaub H, Marcus K. 2021. Quantitative mass spectrometry-based proteomics: an overview. *Methods Mol. Biol.* 2228:85–116
51. Li X, Yang X, Hoang V, Liu Y-H. 2019. Characterization of protein disulfide linkages by MS in-source dissociation comparing to CID and ETD tandem MS. *J. Am. Soc. Mass Spectrom.* 30(3):519–28
52. Liu Y, Li G, Li L. 2021. Targeted top-down mass spectrometry for the characterization and tissue-specific functional discovery of crustacean hyperglycemic hormones (CHH) and CHH precursor-related peptides in response to low pH stress. *J. Am. Soc. Mass Spectrom.* 32(6):1352–60
53. Ankney JA, Muneer A, Chen X. 2018. Relative and absolute quantitation in mass spectrometry-based proteomics. *Annu. Rev. Anal. Chem.* 11:49–77
54. Tillmaand EG, Anapindi KDB, De La Toba EA, Guo CJ, Krebs J, et al. 2020. Quantitative characterization of the neuropeptide level changes in dorsal horn and dorsal root ganglia regions of the murine itch models. *J. Proteome Res.* 19(3):1248–57
55. Ye H, Wang J, Tian Z, Ma F, Dowell J, et al. 2017. Quantitative mass spectrometry reveals food intake-induced neuropeptide level changes in rat brain: functional assessment of selected neuropeptides as feeding regulators. *Mol. Cell. Proteom.* 16(11):1922–37
56. Schilling B, Rardin MJ, MacLean BX, Zawadzka AM, Frewen BE, et al. 2012. Platform-independent and label-free quantitation of proteomic data using MS1 extracted ion chromatograms in skyline: application to protein acetylation and phosphorylation. *Mol. Cell. Proteom.* 11(5):202–14
57. Sauer CS, Li L. 2021. Mass spectrometric profiling of neuropeptides in response to copper toxicity via isobaric tagging. *Chem. Res. Toxicol.* 34(5):1329–36
58. Frost DC, Feng Y, Li L. 2020. 21-Plex DiLeu isobaric tags for high-throughput quantitative proteomics. *Anal. Chem.* 92(12):8228–34
59. Boonen K, De Haes W, Van Houtven J, Verdonck R, Baggerman G, et al. 2018. Quantitative peptidomics with isotopic and isobaric tags. *Methods Mol. Biol.* 1719:141–59
60. Wang X, Shen S, Rasam SS, Qu J. 2019. MS1 ion current-based quantitative proteomics: a promising solution for reliable analysis of large biological cohorts. *Mass Spectrom. Rev.* 38(6):461–82
61. Barkovits K, Pacharra S, Pfeiffer K, Steinbach S, Eisenacher M, et al. 2020. Reproducibility, specificity and accuracy of relative quantification using spectral library-based data-independent acquisition. *Mol. Cell. Proteom.* 19(1):181–97
62. DeLaney K, Li L. 2019. Data independent acquisition mass spectrometry method for improved neuropeptidomic coverage in crustacean neural tissue extracts. *Anal. Chem.* 91(8):5150–58
63. DeLaney K, Hu M, Wu W, Nusbaum MP, Li L. 2022. Mass spectrometry profiling and quantitation of changes in circulating hormones secreted over time in cancer borealis hemolymph due to feeding behavior. *Anal. Bioanal. Chem.* 414(1):533–43

64. Kiontke A, Oliveira-Birkmeier A, Opitz A, Birkemeyer C. 2016. Electrospray ionization efficiency is dependent on different molecular descriptors with respect to solvent pH and instrumental configuration. *PLOS ONE* 11(12):e0167502
65. Hopkins K, Mukherjee S, Ponce D, Mangum J, Jacobson LH, Hoyer D. 2021. Development of a LC-ESI-MRM method for the absolute quantification of orexin A in the CSF of individual mice. *Med. Drug Discov.* 11:100102
66. Morris CB, Poland JC, May JC, McLean JA. 2020. Fundamentals of ion mobility-mass spectrometry for the analysis of biomolecules. *Methods Mol. Biol.* 2084:1–31
67. Mun D-G, Vanderboom PM, Madugundu AK, Garapati K, Chavan S, et al. 2021. DIA-based proteome profiling of nasopharyngeal swabs from COVID-19 patients. *J. Proteome Res.* 20(8):4165–75
68. Pfammatter S, Wu Z, Bonneil E, Bailey DJ, Prasad S, et al. 2021. Integration of segmented ion fractionation and differential ion mobility on a Q-exactive hybrid quadrupole orbitrap mass spectrometer. *Anal. Chem.* 93(28):9817–25
69. Do TD, Checco JW, Tro M, Shea J-E, Bowers MT, Sweedler JV. 2018. Conformational investigation of the structure-activity relationship of GdFFD and its analogues on an achatin-like neuropeptide receptor of *Aplysia californica* involved in the feeding circuit. *Phys. Chem. Chem. Phys.* 20(34):22047–57
70. Bleiholder C, Dupuis NF, Bowers MT. 2013. Dimerization of chirally mutated Enkephalin neurotransmitters: implications for peptide and protein aggregation mechanisms. *J. Phys. Chem. B* 117(6):1770–79
71. Vrkoslav V, Muck A, Brown JM, Hubálek M, Cvačka J. 2018. The matrix-assisted laser desorption/ionisation in-source decay of peptides using ion mobility enabled quadrupole-time-of-flight mass spectrometry. *Rapid Commun. Mass Spectrom.* 32(24):2099–2105
72. Jeanne Dit Fouque K, Moreno J, Fernandez-Lima F. 2019. Exploring the conformational space of growth-hormone-releasing hormone analogues using dopant assisted trapped ion mobility spectrometry-mass spectrometry. *J. Phys. Chem. B* 123(29):6169–77
73. Zhang L, Khattar N, Kemenes I, Kemenes G, Zrinyi Z, et al. 2018. Subcellular peptide localization in single identified neurons by capillary microsampling mass spectrometry. *Sci. Rep.* 8(1):12227
74. Harvey SR, MacPhee CE, Barran PE. 2011. Ion mobility mass spectrometry for peptide analysis. *Methods* 54(4):454–61
75. Paglia G, Astarita G. 2019. Traveling wave ion mobility mass spectrometry: metabolomics applications. *Methods Mol. Biol.* 1978:39–53
76. Meier F, Park MA, Mann M. 2021. Trapped ion mobility spectrometry and parallel accumulation–serial fragmentation in proteomics. *Mol. Cell. Proteom.* 20:100138
77. Spraggins JM, Djambazova KV, Rivera ES, Migas LG, Neumann EK, et al. 2019. High-performance molecular imaging with MALDI trapped ion-mobility time-of-flight (timsTOF) mass spectrometry. *Anal. Chem.* 91(22):14552–60
78. Meier F, Brunner A-D, Koch S, Koch H, Lubeck M, et al. 2018. Online parallel accumulation-serial fragmentation (PASEF) with a novel trapped ion mobility mass spectrometer. *Mol. Cell. Proteom.* 17(12):2534–45
79. Mast DH, Checco JW, Sweedler JV. 2021. Advancing D-amino acid-containing peptide discovery in the metazoan. *Biochim. Biophys. Acta Proteins Proteom.* 1869(1):140553
80. Mast DH, Liao H-W, Romanova EV, Sweedler JV. 2021. Analysis of peptide stereochemistry in single cells by capillary electrophoresis-trapped ion mobility spectrometry mass spectrometry. *Anal. Chem.* 93(15):6205–13
81. Peeters MKR, Baggerman G, Gabriels R, Pepermans E, Menschaert G, Boonen K. 2021. Ion mobility coupled to a time-of-flight mass analyzer combined with fragment intensity predictions improves identification of classical bioactive peptides and small open reading frame-encoded peptides. *Front. Cell Dev. Biol.* 9:720570
82. Willems S, Voytik E, Skowronek P, Strauss MT, Mann M. 2021. Alphatims: indexing trapped ion mobility spectrometry-TOF data for fast and easy accession and visualization. *Mol. Cell. Proteom.* 20:100149
83. Caprioli RM, Farmer TB, Gile J. 1997. Molecular imaging of biological samples: localization of peptides and proteins using MALDI-TOF MS. *Anal. Chem.* 69(23):4751–60

84. Nemes P, Woods AS, Vertes A. 2010. Simultaneous imaging of small metabolites and lipids in rat brain tissues at atmospheric pressure by laser ablation electrospray ionization mass spectrometry. *Anal. Chem.* 82(3):982–88
85. Phan NTN, Mohammadi AS, Dowlatshahi Pour M, Ewing AG. 2016. Laser desorption ionization mass spectrometry imaging of *Drosophila* brain using matrix sublimation versus modification with nanoparticles. *Anal. Chem.* 88(3):1734–41
86. Dill AL, Ifa DR, Manicke NE, Ouyang Z, Cooks RG. 2009. Mass spectrometric imaging of lipids using desorption electrospray ionization. *J. Chromatogr. B* 877(26):2883–89
87. Bergman H-M, Lundin E, Andersson M, Lanekoff I. 2016. Quantitative mass spectrometry imaging of small-molecule neurotransmitters in rat brain tissue sections using nanospray desorption electrospray ionization. *Analyst* 141(12):3686–95
88. Buchberger AR, Vu NQ, Johnson J, DeLaney K, Li L. 2020. A simple and effective sample preparation strategy for MALDI-MS imaging of neuropeptide changes in the crustacean brain due to hypoxia and hypercapnia stress. *J. Am. Soc. Mass Spectrom.* 31(5):1058–65
89. Hulme H, Fridjonsdottir E, Gunnarsdottir H, Vallianatou T, Zhang X, et al. 2020. Simultaneous mass spectrometry imaging of multiple neuropeptides in the brain and alterations induced by experimental parkinsonism and L-DOPA therapy. *Neurobiol. Dis.* 137:104738
90. Pratavieira M, da Silva Menegasso AR, Esteves FG, Sato KU, Malaspina O, Palma MS. 2018. MALDI imaging analysis of neuropeptides in Africanized honeybee (*Apis mellifera*) brain: effect of aggressiveness. *J. Proteome Res.* 17(7):2358–69
91. Habenstein J, Schmitt F, Liessem S, Ly A, Trede D, et al. 2021. Transcriptomic, peptidomic, and mass spectrometry imaging analysis of the brain in the ant *Cataglyphis nodus*. *J. Neurochem.* 158(2):391–412
92. Sui P, Watanabe H, Artemenko K, Sun W, Bakalkin G, et al. 2017. Neuropeptide imaging in rat spinal cord with MALDI-TOF MS: method development for the application in pain-related disease studies. *Eur. J. Mass Spectrom.* 23(3):105–15
93. Vu NQ, Buchberger AR, Johnson J, Li L. 2021. Complementary neuropeptide detection in crustacean brain by mass spectrometry imaging using formalin and alternative aqueous tissue washes. *Anal. Bioanal. Chem.* 413(10):2665–73
94. Li G, Ma F, Cao Q, Zheng Z, DeLaney K, et al. 2019. Nanosecond photochemically promoted click chemistry for enhanced neuropeptide visualization and rapid protein labeling. *Nat. Commun.* 10:4697
95. Paine MRL, Ellis SR, Maloney D, Heeren RMA, Verhaert PDEM. 2018. Digestion-free analysis of peptides from 30-year-old formalin-fixed, paraffin-embedded tissue by mass spectrometry imaging. *Anal. Chem.* 90(15):9272–80
96. Cohen SL, Chait BT. 1996. Influence of matrix solution conditions on the MALDI-MS analysis of peptides and proteins. *Anal. Chem.* 68(1):31–37
97. Römpp A, Spengler B. 2013. Mass spectrometry imaging with high resolution in mass and space. *Histochem. Cell Biol.* 139(6):759–83
98. Ly A, Ragionieri L, Liessem S, Becker M, Deininger S-O, et al. 2019. Enhanced coverage of insect neuropeptides in tissue sections by an optimized mass-spectrometry-imaging protocol. *Anal. Chem.* 91(3):1980–88
99. DeLaney K, Li L. 2020. Neuropeptidomic profiling and localization in the crustacean cardiac ganglion using mass spectrometry imaging with multiple platforms. *J. Am. Soc. Mass Spectrom.* 31(12):2469–78
100. Potočnik NO, Fisher GL, Prop A, Heeren RMA. 2017. Sequencing and identification of endogenous neuropeptides with matrix-enhanced secondary ion mass spectrometry tandem mass spectrometry. *Anal. Chem.* 89(16):8223–27
101. Zavalin A, Yang J, Hayden K, Vestal M, Caprioli RM. 2015. Tissue protein imaging at 1 μm laser spot diameter for high spatial resolution and high imaging speed using transmission geometry MALDI TOF MS. *Anal. Bioanal. Chem.* 407(8):2337–42
102. Kompauer M, Heiles S, Spengler B. 2017. Atmospheric pressure MALDI mass spectrometry imaging of tissues and cells at 1.4-μm lateral resolution. *Nat. Methods* 14(1):90–96
103. Li G, Cao Q, Liu Y, DeLaney K, Tian Z, et al. 2019. Characterizing and alleviating ion suppression effects in atmospheric pressure matrix-assisted laser desorption/ionization. *Rapid Commun. Mass Spectrom.* 33(4):327–35

104. Zhang Y, Buchberger A, Muthuvel G, Li L. 2015. Expression and distribution of neuropeptides in the nervous system of the crab *Carcinus maenas* and their roles in environmental stress. *Proteomics* 15(23–24):3969–79
105. Bivehed E, Strömvall R, Bergquist J, Bakalkin G, Andersson M. 2017. Region-specific bioconversion of dynorphin neuropeptide detected by in situ histochemistry and MALDI imaging mass spectrometry. *Peptides* 87:20–27
106. Ong T-H, Romanova EV, Roberts-Galbraith RH, Yang N, Zimmerman TA, et al. 2016. Mass spectrometry imaging and identification of peptides associated with cephalic ganglia regeneration in *Schmidtea mediterranea*. *J. Biol. Chem.* 291(15):8109–20
107. DeLaney K, Hu M, Hellenbrand T, Dickinson PS, Nusbaum MP, Li L. 2021. Mass spectrometry quantification, localization, and discovery of feeding-related neuropeptides in *Cancer borealis*. *ACS Chem. Neurosci.* 12(4):782–98
108. DeLaney K, Li L. 2020. Capillary electrophoresis coupled to MALDI mass spectrometry imaging with large volume sample stacking injection for improved coverage of *C. borealis* neuropeptidome. *Analyst* 145(1):61–69
109. Cao Q, Wang Y, Chen B, Ma F, Hao L, et al. 2019. Visualization and identification of neurotransmitters in crustacean brain via multifaceted mass spectrometric approaches. *ACS Chem. Neurosci.* 10(3):1222–29
110. Shariatgorji M, Nilsson A, Källback P, Karlsson O, Zhang X, et al. 2015. Pyrylium salts as reactive matrices for MALDI-MS imaging of biologically active primary amines. *J. Am. Soc. Mass Spectrom.* 26(6):934–39
111. Kulkarni A, Anderson AG, Merullo DP, Konopka G. 2019. Beyond bulk: a review of single cell transcriptomics methodologies and applications. *Curr. Opin. Biotechnol.* 58:129–36
112. Liessem S, Ragionieri L, Neupert S, Büschges A, Predel R. 2018. Transcriptomic and neuropeptidomic analysis of the stick insect, *Carausius morosus*. *J. Proteome Res.* 17(6):2192–2204
113. Comi TJ, Do TD, Rubakhin SS, Sweedler JV. 2017. Categorizing cells on the basis of their chemical profiles: progress in single-cell mass spectrometry. *J. Am. Chem. Soc.* 139(11):3920–29
114. Zhang G, Yuan W, Vilim FS, Romanova EV, Yu K, et al. 2018. Newly identified *Aplysia* SPTR-gene family-derived peptides: localization and function. *ACS Chem. Neurosci.* 9(8):2041–53
115. Zhang G, Vilim FS, Liu D-D, Romanova EV, Yu K, et al. 2017. Discovery of leucokinin-like neuropeptides that modulate a specific parameter of feeding motor programs in the molluscan model, *Aplysia*. *J. Biol. Chem.* 292(46):18775–89
116. Lee CY, Fan Y, Rubakhin SS, Yoon S, Sweedler JV. 2016. A neuron-in-capillary platform for facile collection and mass spectrometric characterization of a secreted neuropeptide. *Sci. Rep.* 6(1):26940
117. Do TD, Ellis JF, Neumann EK, Comi TJ, Tillmaand EG, et al. 2018. Optically guided single cell mass spectrometry of rat dorsal root ganglia to profile lipids, peptides and proteins. *ChemPhysChem* 19(10):1180–91
118. Jansson ET, Comi TJ, Rubakhin SS, Sweedler JV. 2016. Single cell peptide heterogeneity of rat islets of langerhans. *ACS Chem. Biol.* 11(9):2588–95
119. Ong T-H, Kissick DJ, Jansson ET, Comi TJ, Romanova EV, et al. 2015. Classification of large cellular populations and discovery of rare cells using single cell matrix-assisted laser desorption/ionization time-of-flight mass spectrometry. *Anal. Chem.* 87(14):7036–42
120. Rubakhin SS, Sweedler JV. 2007. Characterizing peptides in individual mammalian cells using mass spectrometry. *Nat. Protoc.* 2(8):1987–97
121. Comi TJ, Neumann EK, Do TD, Sweedler JV. 2017. microMS: a Python platform for image-guided mass spectrometry profiling. *J. Am. Soc. Mass Spectrom.* 28(9):1919–28
122. Neumann EK, Ellis JF, Triplett AE, Rubakhin SS, Sweedler JV. 2019. Lipid analysis of 30 000 individual rodent cerebellar cells using high-resolution mass spectrometry. *Anal. Chem.* 91(12):7871–78
123. Xie YR, Castro DC, Bell SE, Rubakhin SS, Sweedler JV. 2020. Single-cell classification using mass spectrometry through interpretable machine learning. *Anal. Chem.* 92(13):9338–47
124. Masuda-Nakagawa LM, Ito K, Awasaki T, O'Kane CJ. 2014. A single GABAergic neuron mediates feedback of odor-evoked signals in the mushroom body of larval *Drosophila*. *Front. Neural Circuits* 8:35
125. Page JS, Rubakhin SS, Sweedler JV. 2002. Single-neuron analysis using CE combined with MALDI MS and radionuclide detection. *Anal. Chem.* 74(3):497–503

126. Neupert S, Fusca D, Kloppenburg P, Predel R. 2018. Analysis of single neurons by perforated patch clamp recordings and MALDI-TOF mass spectrometry. *ACS Chem. Neurosci.* 9(8):2089–96
127. Comi TJ, Makurath MA, Philip MC, Rubakhin SS, Sweedler JV. 2017. MALDI MS guided liquid microjunction extraction for capillary electrophoresis-electrospray ionization MS analysis of single pancreatic islet cells. *Anal. Chem.* 89(14):7765–72
128. Fisher JM, Sossin W, Newcomb R, Scheller RH. 1988. Multiple neuropeptides derived from a common precursor are differentially packaged and transported. *Cell* 54(6):813–22
129. Fumagalli G, Zanini A. 1985. In cow anterior pituitary, growth hormone and prolactin can be packed in separate granules of the same cell. *J. Cell Biol.* 100(6):2019–24
130. Bonnin EA, Rizzoli SO. 2020. Novel secondary ion mass spectrometry methods for the examination of metabolic effects at the cellular and subcellular levels. *Front. Behav. Neurosci.* 14:124
131. Altelaar AFM, van Minnen J, Jiménez CR, Heeren RMA, Piersma SR. 2005. Direct molecular imaging of *Lymnaea stagnalis* nervous tissue at subcellular spatial resolution by mass spectrometry. *Anal. Chem.* 77(3):735–41
132. Jiang Z, Lietz CB, Podvin S, Yoon MC, Toneff T, et al. 2021. Differential neuropeptidomes of dense core secretory vesicles (DCSV) produced at intravesicular and extracellular pH conditions by proteolytic processing. *ACS Chem. Neurosci.* 12(13):2385–98
133. Rubakhin SS, Garden RW, Fuller RR, Sweedler JV. 2000. Measuring the peptides in individual organelles with mass spectrometry. *Nat. Biotechnol.* 18(2):172–75
134. Castro DC, Xie YR, Rubakhin SS, Romanova EV, Sweedler JV. 2021. Image-guided MALDI mass spectrometry for high-throughput single-organelle characterization. *Nat. Methods* 18:1233–38
135. Rubakhin SS, Churchill JD, Greenough WT, Sweedler JV. 2006. Profiling signaling peptides in single mammalian cells using mass spectrometry. *Anal. Chem.* 78(20):7267–72
136. Rubakhin SS, Greenough WT, Sweedler JV. 2003. Spatial profiling with MALDI MS: distribution of neuropeptides within single neurons. *Anal. Chem.* 75(20):5374–80
137. Rubakhin SS, Sweedler JV. 2008. Quantitative measurements of cell–cell signaling peptides with single-cell MALDI MS. *Anal. Chem.* 80(18):7128–36

Annual Review of Analytical Chemistry

Volume 15, 2022

Contents

Errata

An online log of corrections to *Annual Review of Analytical Chemistry* articles may be found at http://www.annualreviews.org/errata/anchem